

Explainable Preference Learning: a Decision Tree-based Surrogate Model for Preferential Bayesian Optimization

Nick Leenders ^{*1 2 3} Thomas Quadt ^{*1 2} Boris Čule ¹ Roy Lindelauf ^{1 2} Herman Monsuur ² Joost van Oijen ³
Mark Voskuyl ²

Abstract

Current Preferential Bayesian Optimization methods rely on Gaussian Processes (GPs) as surrogate models. These models are hard to interpret, struggle with handling categorical data, and are computationally complex, limiting their real-world usability. In this paper, we introduce an inherently interpretable decision tree-based surrogate model capable of handling both categorical and continuous data, and scalable to large datasets. Extensive numerical experiments on eight increasingly spiky optimization functions show that our model outperforms GP-based alternatives on spiky functions and has only marginally lower performance for non-spiky functions. Moreover, we apply our model to the real-world Sushi dataset and show its ability to learn an individual’s sushi preferences. Finally, we show some initial work on using historical preference data to speed up the optimization process for new unseen users.

1. Introduction

Preferential Bayesian Optimization (PBO) is a sample-efficient approach for finding the maximum of an unknown function using only pairwise comparisons (PCs) (González et al., 2017). This setting occurs in decision-making tasks, where a decision-maker’s (DM’s) preferences are modeled via a latent utility function. To find the DM’s most preferred solution, one needs to find the maximum of this utility function. This function cannot be accessed directly as it is difficult for a DM to assign absolute numerical ratings to instances (Zintgraf et al., 2018). For example, why rate the

^{*}Equal contribution ¹Department of Intelligent Systems, Tilburg University, Tilburg, The Netherlands ²Data Science Center of Excellence, Netherlands Defense Academy, Breda, The Netherlands ³NLR - Royal Netherlands Aerospace Centre, Amsterdam, The Netherlands. Correspondence to: Nick Leenders <nick.leenders@nlr.nl>, Thomas Quadt <t.j.quadt@tilburguniversity.edu>.

Preprint. December 17, 2025.

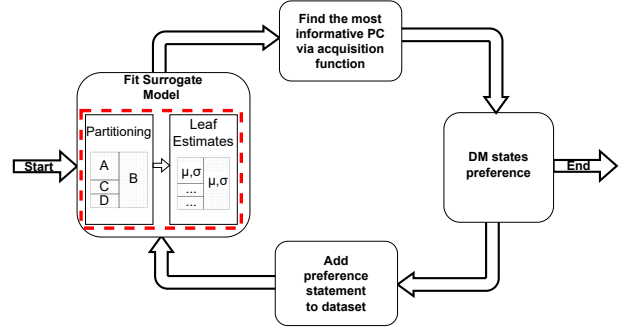


Figure 1. A schematic overview of the PBO loop with the tree-based surrogate model being depicted in the red rectangle. At the start of the process, randomly sampled initial comparisons are asked to the decision-maker and the model is fitted. The process ends when the decision-maker is satisfied with the final solution.

taste of a slice of cake as 7? Why not 8? On the other hand, expressing preferences through pairwise comparisons (e.g., preferring chocolate cake over carrot cake) is cognitively much easier (Larichev, 1992; Greco et al., 2008).

PBO’s optimization loop, as shown in Figure 1, constructs a probabilistic surrogate model of the utility function, based on this probabilistic estimate an acquisition function identifies the most promising next PC to evaluate, performs the evaluation, and reconstructs the surrogate model based on the newly added data. First proposed by Chu & Ghahramani (2005), Gaussian Processes (GPs) have become the standard surrogate model. These models form a probabilistic estimate of the utility function via a kernel function measuring the similarity between points. Over the years, researchers have developed new acquisition functions (e.g., González et al. (2017); Fauvel & Chalk (2021); Astudillo et al. (2023)) and new methods to infer the intractable posterior distribution to train GPs on PC data (e.g., Nielsen et al. (2015); Siivola et al. (2021); Benavoli et al. (2021); Takeno et al. (2023)). To the best of our knowledge, alternative surrogate models, however, have not yet been explored.

Addressing this is important because GPs have several practical limitations. First, GPs become difficult to interpret unless the kernel function is explicitly constrained to be additive over the input dimensions (Plate, 1999). Without such

constraints, GPs behave as black box models, making it hard for DMs to understand why certain solutions are preferred, a critical issue in many real-world applications. Second, GPs struggle with handling qualitative data, especially when a qualitative factor contains many categories (Lin et al., 2024). Discrete data namely introduces discontinuities in the utility function, as the function values will now only change at discrete points. The most commonly used Radial Basis Function kernel and Matérn 2.5 kernels encode inherent smoothness assumptions (infinitely differentiable and twice differentiable, respectively) (Rasmussen & Williams, 2005) and are therefore incapable of modeling these discontinuities. Note that even without discrete data, the utility function can exhibit discontinuities (Gilboa et al., 2020).

Instead of a GP-based surrogate model, we propose to use a tree-based surrogate model, as Decision Trees (DTs) are inherently interpretable, able to capture discontinuities, and well suited for categorical data. To use a DT as a surrogate model for PBO, it needs to provide a probabilistic estimate of the utility function and be learned solely from PC data. Additionally, to retain a high degree of interpretability, a single decision tree with probabilistic leaves is preferred over a completely probabilistic tree. Following these requirements, we thus propose a novel method of learning DTs with probabilistic leaves on PC data. We compare our model to two state-of-the-art GP-based models on eight increasingly spiky benchmark optimization functions and the results show that our model performs slightly worse on non-spiky optimization function but outperforms GP-based models on spiky functions. Moreover, our model scales much better on dataset size, making PBO possible on large datasets. A case study on the existing mixed-type Sushi dataset shows not only the high degree of interpretability of our proposed tree-based surrogate model as well as its capability of handling both qualitative and quantitative data out-of-the-box. Finally, we show some initial work on using historic preference data to speed up the learning process for new unseen decision-makers.

Our code is available at <https://github.com/Thomasq99/DT-PBO>.

2. Background

2.1. Preferential Bayesian Optimization

In PBO, a DM’s preferences are modeled by a latent utility function $f : \mathcal{X} \rightarrow \mathbb{R}$, where $\mathcal{X} = \mathcal{X}_{cont} \times \mathcal{X}_{cat}$, with $\mathcal{X}_{cont} \subseteq \mathbb{R}^{d_c}$, and $\mathcal{X}_{cat} = C_1 \times \dots \times C_{d_k}$, where each C_i is a finite set of category labels. In particular, f measures the degree of preference of a solution \mathbf{x} , where if \mathbf{x} is preferred to \mathbf{x}' , $f(\mathbf{x}) > f(\mathbf{x}')$. The DM’s most preferred solution \mathbf{x}_{MPS} can then be found by solving the global optimization problem $\mathbf{x}_{MPS} = \arg \max_{\mathbf{x} \in \mathcal{X}} f(\mathbf{x})$.

The main premise in PBO is that f is not observed directly. Instead, f is observed via PCs $(\mathbf{x}, \mathbf{x}') \in \mathcal{X} \times \mathcal{X}$ from which we observe preference relations $\mathbf{x} \succ \mathbf{x}'$ indicating that \mathbf{x} is preferred to \mathbf{x}' . The goal is to find \mathbf{x}_{MPS} in as few PCs as possible.

To this end, as shown in Figure 1, PBO iteratively selects new pairs to query, updates a probabilistic surrogate model over f based on the observed preferences, and uses this model to guide future comparisons. Specifically, PBO starts with specifying a prior belief over the unknown function f . Then, after observing t preference relations, $\mathcal{D}_t = \{\mathbf{x}_i \succ \mathbf{x}'_i\}_{i=1}^t$, the likelihood $p(\mathcal{D}_t | f)$ and prior $p(f)$ are used to find the posterior $p(f | \mathcal{D}_t)$ via Bayes’ rule. This posterior is then used to select the next pair $(\mathbf{x}_{t+1}, \mathbf{x}'_{t+1})$ by maximizing an acquisition function $a(\mathbf{x}, \mathbf{x}' | \mathcal{D}_t)$ designed to trade off exploration and exploitation. The DM evaluates the new pair, and the observed preference statement is added to the data. This loop of querying, updating, and selecting new pairs continues until a stopping criterion is met.

2.2. Preference Learning with Gaussian Processes

Let $\mathcal{D}_n = \{\mathbf{x}_i \succ \mathbf{x}'_i\}_{i=1}^n$ be a set of n preference relations formed from m unique instances $\{\mathbf{x}_1, \dots, \mathbf{x}_m\} \subseteq \mathcal{X}^n$. The main idea is to define a GP prior over the latent function f , use a pairwise likelihood function, and find the posterior using Bayes’ rule.

GP Prior: A Gaussian Process (Williams & Rasmussen, 1995) defines a distribution over functions $f \sim \mathcal{GP}(m(\mathbf{x}), \mathcal{K}_\theta(\mathbf{x}, \mathbf{x}'))$, where $m(\mathbf{x})$ is the mean function and $\mathcal{K}_\theta(\mathbf{x}, \mathbf{x}')$ is a parametrized kernel function encoding assumptions about the smoothness or form of the function f . In preference learning, zero-mean GP priors are used, which model the latent function values $f(\mathbf{x}_i)$ as a multivariate joint Gaussian

$$p(\mathbf{f}) = \frac{1}{(2\pi)^{\frac{m}{2}} |\Sigma|^{\frac{1}{2}}} \exp\left(-\frac{1}{2} \mathbf{f}^\top \Sigma^{-1} \mathbf{f}\right), \quad (1)$$

where Σ is an $m \times m$ covariance matrix with entries $\Sigma_{ij} = \mathcal{K}_\theta(\mathbf{x}_i, \mathbf{x}_j)$, and $\mathbf{f} = [f(\mathbf{x}_1), \dots, f(\mathbf{x}_m)]^\top$.

Pairwise Likelihood: Assuming that observations are influenced by homoskedastic Gaussian noise and assuming independence of preference statements, following Benavoli & Azzimonti (2024) the likelihood of observing n preference relations \mathcal{D}_n given \mathbf{f} is

$$p(\mathcal{D}_n | \mathbf{f}) = \prod_i^n \Phi\left(\frac{f(\mathbf{x}_i) - f(\mathbf{x}'_i)}{\sqrt{2}\sigma_{noise}}\right), \quad (2)$$

where $\Phi(z) = \int_{-\infty}^z \mathcal{N}(\mathbf{x}; 0, 1) d\mathbf{x}$ is the cumulative standard normal distribution.

Posterior: The posterior can be found using Bayes' rule

$$p(\mathbf{f}|\mathcal{D}) = \frac{p(\mathcal{D}|\mathbf{f})p(\mathbf{f})}{p(\mathcal{D})},$$

where the prior $p(\mathbf{f})$ is defined in Equation 1, the likelihood $p(\mathcal{D}|\mathbf{f})$ is defined in Equation 2, and the normalization factor $p(\mathcal{D}) = \int p(\mathcal{D}|\mathbf{f})p(\mathbf{f})d\mathbf{f}$. The latter is only needed for model selection.

This posterior is a computationally intractable skew GP (Benavoli et al., 2021). There exist two approaches to deal with this. First, most commonly used, one can approximate the posterior with a Gaussian using, for example, Laplace Approximation (LA) (Chu & Ghahramani, 2005) or Expectation Propagation (Minka, 2001). Alternatively, one can use Markov chain Monte Carlo methods to employ the skew GP directly. In this research, LA is used because of its computational simplicity. The use of different approximation methods is left for future research.

In LA, the posterior is approximated by a Gaussian centered at the mode (i.e., maximum a posteriori (MAP) estimate) of the posterior (Chu & Ghahramani, 2005). In particular, $\mathbf{f}|\mathcal{D} \sim \mathcal{N}(\mathbf{f}_{MAP}, \Sigma_{post})$ where $\mathbf{f}_{MAP} = \arg \max_{\mathbf{f}} p(\mathbf{f}|\mathcal{D})$, which can be found as minimizer of the following functional

$$L(\mathbf{f}) = - \sum_{i=1}^n \ln \Phi\left(\frac{f(x_i) - f(x'_i)}{\sqrt{2}\sigma_{noise}}\right) + \frac{1}{2} \mathbf{f}^\top \Sigma^{-1} \mathbf{f}. \quad (3)$$

The posterior covariance Σ_{post} is the Hessian of $L(\mathbf{f})$ evaluated at the MAP estimate

$$\Sigma_{post}^{-1} = H(L(\mathbf{f}))|_{\mathbf{f}=\mathbf{f}_{MAP}} = (\Sigma^{-1} + \Lambda_{MAP}), \quad (4)$$

where Λ is an $m \times m$ matrix where the ij th element is $\frac{\partial^2 \sum_{k=1}^n -\ln \Phi(z_k)}{\partial f(x_i) \partial f(x_j)}$, $z_k = \frac{f_{MAP}(x_k) - f_{MAP}(x'_k)}{\sqrt{2}\sigma_{noise}}$.

2.3. Extending Decision Trees to Pairwise data

A simplistic approach to training a decision tree with PCs would be to frame it as a classification problem, where the tree is trained on (*Item A*, *Item B*, *User prefers A*) as is done by Qomariyah et al. (2020). There are a few problems with this approach. Firstly, this would lead to an asymmetrical model. The only way to solve this is to train on both $(A, B) \rightarrow 1$ and $(B, A) \rightarrow 0$ for every single comparison. This doubles the dataset and forces the tree to learn two separate rules for the same underlying preference, which is highly inefficient. Instead, as done by Shavarani et al. (2023), one could use the difference as input for the tree and train the tree as follows: if $(A - B) > 0.5$ A is preferred, else B. However, this would lead to loss of the context of

the absolute feature values. These approaches provide only local interpretability: one can determine when one item is preferred over another, while global interpretability is not possible, as one cannot easily see which item is overall the best or second-best. Finally, neither one of these methods provide a probabilistic estimate and both are therefore not suitable for active learning. Although, Shavarani et al. (2025) extend their method to be suitable for active learning by using Random Forest models, this comes at the cost of interpretability.

Somewhat similar to learning from PC data is learning from ranking data, i.e., data where items are ordered by preference or outcome rather than assigned absolute values. An approach that uses DTs to learn directly from ranking data is introduced by Cheng et al. (2009). The model uses a ranking probability model (Mallows model) at every potential split to find a split value that partitions the data into the most homogeneous subgroups of rankings. This method would be suitable for active learning, although Mallows model is computationally expensive. However, this method is made for label preferences, where the training data consists of pairwise comparisons among labels associated with the objects, whereas in our research we focus on object preferences instead, where the training data consists of pairwise comparisons among the characteristics or attributes associated with the objects (Benavoli & Azzimonti, 2024). Similarly, Rebelo & Soares (2008) build a tree directly from ranking data. Although, their method is correlation-based rather than probabilistic, making it unsuitable for active learning. The splits are determined by finding the attribute that maximizes the intra-cluster similarity of the resulting subsets, where similarity is measured by the average Spearman's rank correlation coefficient. Finally, Liu & Shih (2016) transform the PCs into a scoring vector using a scoring system. Each object receives a point whenever it is preferred to another object. The preference learning problem is now re-framed as a multi-response regression task, the higher the score, the more preferred the object is, leading to a regression tree. This method also lacks a probabilistic estimate and is therefore not suitable for active learning.

Note that while probabilistic extensions of DTs, such as Bayesian DTs (e.g., Chipman et al. (1998); Nuti et al. (2021)) exist, these methods are not applicable to PCs yet. In conclusion, a truly interpretable sample-efficient DT should provide a probabilistic estimate of the preference value in each leaf. Additionally, to be cognitively easy to use for the DM, it should be trained on object PC data. To the best of our knowledge, no such method exists.

3. Method

As shown in Figure 1, our proposed method for PBO follows the same optimization loop as the GP-based alterna-

tives. However, instead of a GP, we propose to use a tree-based surrogate model which is fitted on the current set of preference statements in two steps. First, as explained in Section 3.1, the space is partitioned into a set of leaves using a novel splitting heuristic. Second, as explained in Section 3.2, for each leaf, a Gaussian is fitted to represent the prediction estimate. The resulting surrogate model is a single decision tree with Gaussian distributions as probabilistic preference value predictions in each leaf. After fitting the surrogate model, our proposed method uses the Expected Utility of Best Option (qEUBO) (Astudillo et al., 2023) acquisition function to find the most informative PC to ask (see Section 3.3 for details).

3.1. Partitioning the Space

First, to learn a single regression tree with probabilistic leaves from PC data, we need a new splitting heuristic. The idea proposed here is the Consistency Score (defined in Equation 5), a metric designed to find a split between winners and losers from PCs. For a given node containing a set of k comparison pairs $D = \{(\mathbf{x}_i^w, \mathbf{x}_i^l)\}_{i=1}^k$, where \mathbf{x}^w is the "winner" and \mathbf{x}^l is the "loser", we search for the optimal split. A split is defined by a feature index k and a threshold value t , where $\mathbf{x}[k]$ is the k^{th} feature value. We define two counts: n_{right} for the pairs where the winner is placed on the right side of the split and the loser on the left, and n_{left} for the reverse case. This gives the following:

$$\begin{aligned} n_{\text{right}}(k, t) &= |(\mathbf{x}^w, \mathbf{x}^l) \in D \mid \mathbf{x}^w[k] \geq t \wedge \mathbf{x}^l[k] < t| \\ n_{\text{left}}(k, t) &= |(\mathbf{x}^w, \mathbf{x}^l) \in D \mid \mathbf{x}^w[k] < t \wedge \mathbf{x}^l[k] \geq t| \end{aligned}$$

The consistency score (S_c) can then be found as:

$$S_c(k, t) = |n_{\text{right}}(k, t) - n_{\text{left}}(k, t)|. \quad (5)$$

Essentially, this score rates how well winners are separated from losers, where a high $S_c(k, t)$ indicates that the split aligns well with observed preferences, separating winners and losers across the threshold. The tree is then constructed by greedily finding the split k^*, t^* that maximizes the score. This method is different from the approaches mentioned in Section 2.3, which are based on ranking algorithms. Rather than transforming the data, our method trains directly on preference pairs $(\mathbf{x}^w, \mathbf{x}^l)$.

The growth of the decision tree is controlled by several hyperparameters that serve to prevent overfitting and control the model's complexity. First, *minimum split score*: a node will only split if the best possible score $S_c(k^*, t^*)$ is greater than this hyperparameter. If not, the node will become a leaf. This prevents the tree from making splits that are not informative enough or are likely based on noise. Secondly, a node is only considered for splitting if the number of comparison pairs it contains, $|D|$, is at least the value of the *minimum samples before split* hyperparameter. This

prevents the model from overfitting on very small subsets of data. Finally, the *max depth* hyperparameter imposes a hard limit on the maximum number of levels in the tree. Any node reaching this depth is automatically converted into a leaf, regardless of any other criteria. This ensures the tree remains small enough to be interpretable.

After a split, the child node datasets D_{left} and D_{right} are formed only by pairs that fall entirely on one side of the partition:

$$\begin{aligned} D_{\text{left}} &= \{(\mathbf{x}^w, \mathbf{x}^l) \in D \mid \mathbf{x}^w[k^*] < t^* \wedge \mathbf{x}^l[k^*] < t^*\} \\ D_{\text{right}} &= \{(\mathbf{x}^w, \mathbf{x}^l) \in D \mid \mathbf{x}^w[k^*] \geq t^* \wedge \mathbf{x}^l[k^*] \geq t^*\} \end{aligned} \quad (6)$$

Note that only pairs whose winner and loser both fall on the same side of the threshold are passed to the corresponding child node. Pairs that straddle the split are discarded, since they provide conflicting information for that threshold. Although this procedure removes some data, it ensures that each child node contains internally consistent comparisons, resulting in purer partitions and shallower, more interpretable trees, removing the need for pruning. This poses a problem, however, for higher dimensional functions ($d > 10$), as straddlers are discarded even though they might still contain relevant information on other dimensions. Potentially this could be solved by not discarding the straddlers, but removing the dimension that was split on out of the consistency score calculation for those comparisons in child nodes instead. This is left as future work.

3.2. Estimating the Leaf Parameters

After observing n preference relations, the latent utility function is represented by m leaf values $\mathbf{f} = [f_1, \dots, f_m]^T$, where each f_j denotes the mean preference value of leaf j . To find the probabilistic leaf estimates, we model them as a joint multivariate Gaussian. To do so, we employ the same Bayesian approach used for GPs. More particularly, as a prior, we assume that each leaf f_j follows an independent zero-mean normal distribution with variance σ_{prior}^2 . Therefore, all leaves follow the joint multivariate Gaussian

$$p(\mathbf{f}) \sim \prod_{j=1}^m \mathcal{N}(0, \sigma_{\text{prior}}^2) = \mathcal{N}(\mathbf{0}, \sigma_{\text{prior}}^2 \mathbf{I}), \quad (7)$$

where \mathbf{I} is the m -dimensional identity matrix. We approximate the posterior with a Gaussian centered at the MAP estimate $\mathbf{f}|D \sim \mathcal{N}(f_{\text{MAP}}, \Sigma_{\text{post}})$ via LA. We use the same pairwise likelihood function defined in Equation 2 as in the GP case but replace the GP prior, with the independent normal prior defined in Equation 7. Therefore, to find the MAP-estimate \mathbf{f}_{MAP} as the minimizer of the functional $L(\mathbf{f})$, we need only change the prior term in Equation 3. The new functional $L(\mathbf{f})$ is thus defined as

$$L(\mathbf{f}) = - \sum_{i=1}^n \ln \Phi\left(\frac{f(x_i) - f(x'_i)}{\sqrt{2}\sigma_{noise}}\right) + \frac{1}{2\sigma_{prior}^2} \mathbf{f}^\top \mathbf{f}.$$

Similarly the posterior covariance becomes

$$\Sigma_{post}^{-1} = H(L(\mathbf{f}))|_{\mathbf{f}=\mathbf{f}_{MAP}} = \left(\frac{1}{\sigma_{prior}^2} I + \Lambda_{MAP}\right), \quad (8)$$

where Λ_{MAP} is as defined in Equation 4.

Note that this method has two hyperparameters σ_{noise} and σ_{prior} . A high σ_{noise} means that the model expects more inconsistencies within the pairwise comparisons and therefore needs a higher absolute difference in the leaf values to get the same predicted probability of item \mathbf{x} being preferred to \mathbf{x}' . σ_{prior} determines the uncertainty of the prior. A low σ_{prior} means that the prior is more certain, and the model needs more proof to deviate from the prior. Additionally, note that when both items of a comparison fall in the same leaf, they share the same latent value f_j , resulting in $P(x > x') = \Phi(0) = 0.5$ for each value f . Such pairs provide no gradient information on $L(\mathbf{f})$ w.r.t. f , and thus do not influence the MAP-estimate and can be discarded from the computation.

Finally, the pairwise likelihood defined in Equation 2 is *translationally invariant* with respect to \mathbf{f} . That is, adding a constant shift c to all components of \mathbf{f} does not influence the pairwise differences and thus leaves the likelihood unchanged. This invariance causes two problems: First, it introduces a large irreducible variance term in the uncertainty estimate. Secondly, it causes a singular or ill-conditioned Hessian. To remedy these issues, the model is made identifiable by adding a sum-to-zero constraint: $\sum_{i=1}^m f = \mathbf{1}\mathbf{f} = 0$. Essentially, this fixes the scale of the model, preventing a constant shift, and thereby removing any variance coming from this. This constraint is incorporated by using Eaton's (Eaton, 1983) normal conditional distribution result, by conditioning the posterior on $\mathbf{1}\mathbf{f} = 0$, where $\mathbf{1}$ is the m -dimensional all-ones vector. The posterior then follows a conditional distribution $p(\mathbf{f}|\mathbf{1}\mathbf{f} = 0, \mathcal{D})$ (for more information see Appendix A)

$$\mathbf{f} \mid \mathbf{1}\mathbf{f} = 0 \sim \mathcal{N}\left(\boldsymbol{\mu}_{cond}, \Sigma_{cond}\right), \quad (9)$$

where

$$\boldsymbol{\mu}_{cond} = \boldsymbol{\mu} - \frac{\mathbf{1}^\top \boldsymbol{\mu}}{\mathbf{1}^\top \Sigma \mathbf{1}} \Sigma \mathbf{1},$$

$$\Sigma_{cond} = \Sigma - \frac{1}{\mathbf{1}^\top \Sigma \mathbf{1}} (\Sigma \mathbf{1})(\Sigma \mathbf{1})^\top.$$

3.3. Active Learning

Similar to regression or classification problems, acquisition functions are used for active learning from PCs. However, instead of evaluating the most informative point, the most informative PC has to be chosen. A common method is to use regular acquisition functions, such as Expected Improvement or Upper Confidence Bound, to find the next best point and compare it to another point (such as the current best), as done by Brochu et al. (2010), Siivola et al. (2021), and Takeno et al. (2023). Another approach is to use specialized acquisition functions for PCs that directly selects the most informative pair to present to the DM. Some examples of these specialized acquisition functions are Expected Improvement under Utility Uncertainty (EI-UU) (Astudillo & Frazier, 2020), Dueling Thompson Sampling (González et al., 2017) and the expected utility of the best option (qEUBO) (Astudillo et al., 2023), which is the method used in this research. The qEUBO acquisition function directly targets PC data. For each candidate pair (x, x') we approximate the expected improvement in utility using the leaf-wise Gaussian predictions (f_{MAP}, σ_{post}) . Specifically, if x and x' belong to leaves i and j , their predictive means and variances are used to evaluate the qEUBO acquisition value to select comparisons expected to yield the highest improvement in the utility of the best option after the query $((\mathbf{x}_{t+1}, \mathbf{x}'_{t+1}) = \arg \max_{\mathbf{x} \in \mathcal{X}} qEUBO(\mathbf{x}, \mathbf{x}'))$. This makes it explicitly formulated for the preference learning setting, rather than adapting standard acquisition functions designed for direct function evaluations. qEUBO has generally achieved good results in PBO. One downside of qEUBO for DTs is that when both items of a candidate pair (y_1, y_2) fall into the same leaf $\mathbb{E}[g(y_1) - g(y_2)] = 0$ and $\sigma^2(y_1, y_2) = 0$, leading to slightly lower values for $qEUBO(y_1, y_2)$, which leads qEUBO to undervalue within-leaf comparisons. To solve this, an option to prioritize within leaf comparisons is added.

4. Numerical Experiments

The goal of these experiments is to evaluate how well the proposed decision-tree performs relative to established GP-based PBO methods, in optimization quality and computational efficiency. We specifically test whether the DT model, which is inherently interpretable and captures discontinuities and categorical effects, can match GP performance on non-spiky functions and outperform it on spiky ones. With "spikiness" we refer to both the frequency and strength of sudden, sharp changes in function value (i.e., spikes). The surface plots in Appendix B show each function's spikiness. To evaluate this, we compare our method to two state-of-the-art methods: SkewGP with Hallucination Believer - Expected Improvement (HB-EI) and LA-based GP with qEUBO. For SkewGP with HB-EI, the implementation

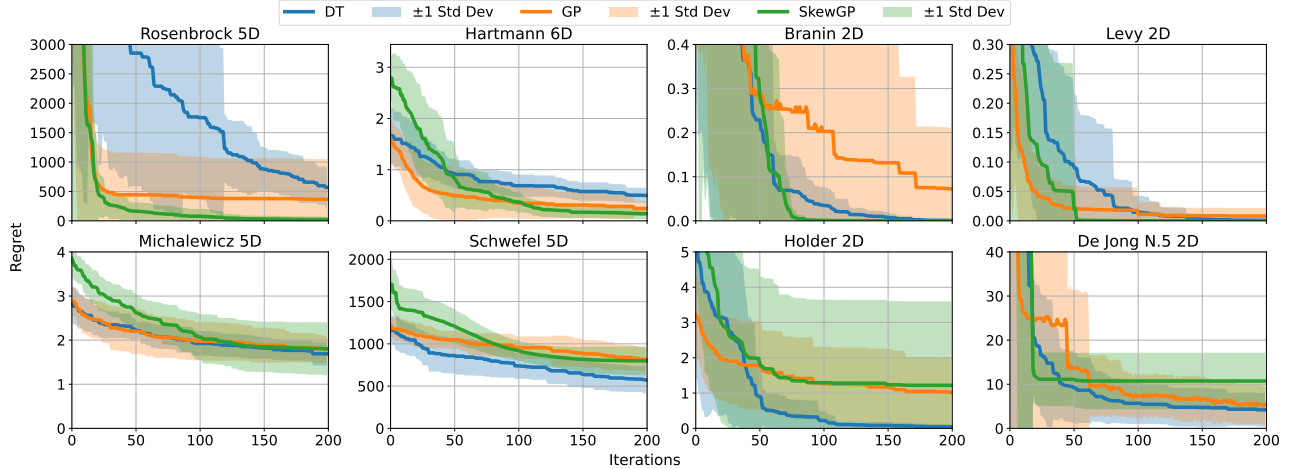


Figure 2. Average Regret over 20 runs of the DT-qEUBO, GP-qEUBO and SkewGP with HB-EI models. The methods are tested on, from left to right, top to bottom, eight increasingly spiky benchmark functions.

of [Takeno et al. \(2023\)](#) is used and for GP the implementation in Botorch ([Balandat et al., 2020](#)) is used. Since the implementations of qEUBO and SkewGP are incompatible due to package dependencies, the comparison to SkewGP-qEUBO cannot be made easily. For both GP-based models, a Radial Basis Function kernel with automatic relevance determination is used. For GP the lengthscales are selected by marginal maximum likelihood estimation after each iteration, whereas for SkewGP this is done every 10 iterations due to the high computational complexity. For each model, the recommendation point x_t is the point $x \in \mathcal{D}_t$ with the highest utility so far. The hyperparameter settings of our DT model are $\sigma_{noise} = 0.01$, $\sigma_{prior} = 0.02$, *min samples split* is 1, *max depth* is 50, and *min split score* is 1 for each experiment. Note that the tree-structure hyperparameters are set to such a value that they are never reached. Instead, the discarding of data controls the depth of the tree automatically. The σ_{noise} and σ_{prior} were chosen based on some initial experiments which showed good results when $\sigma_{noise} \approx \sigma_{prior}$.

The performance of all three models is compared on eight 2D to 6D benchmark functions in increasing order of spikiness. Each model's performance is averaged over 20 runs, varying the initial questions asked to get a robust estimate of the performance. As a performance metric, the regret, which is defined as $f(x^*) - f(\hat{x}_t)$, where $f(x^*)$ is the optimum (maximum) of function f and $f(\hat{x}_t)$ is the model's recommendation point at timestep t , is used. All models start with 20 initial comparisons sampled via Latin Hypercube Sampling ([McKay et al., 1979](#)). In Figure 2, from left to right, top to bottom, the optimization functions get increasingly spiky. In the top row, all relatively non-spiky optimization functions, skewGP generally outperforms both GP and DT. For Branin and Levy, SkewGP converges faster to the op-

timum than DT. GP, on the other hand, never reaches the optimum. Looking at the bottom row, DT performs much better. For Michalewicz, all methods perform equally well, but starting from Schwefel 5D, DT starts to outperform GP and SkewGP. This is caused by the performance degradation for GP and SkewGP on spiky optimization functions because their kernel enforces smoothness. A different kernel with a less strict smoothness assumption could be used, but the shape of the utility function is not known beforehand. Besides, choosing or constructing the right kernel for each function is non-trivial. Looking at the higher-dimensional functions Michalewicz, Rosenbrock, Hartmann, and Schwefel the GP methods perform better on the non-spiky functions whereas the DT-based method performs better on the spiky functions. All methods are thus capable of handling at least 6-dimensional functions. In conclusion, the decision-tree-based method performs better on spiky optimization functions, whereas GP-based models perform better on non-spiky functions. Since, as explained before, real-world utility functions can exhibit discontinuities, good performance on spiky optimization benchmarks is promising for real-life use-cases.

Another advantage of our model is its low running time. Figure 3 shows the cumulative running time needed for 200 iterations on two benchmark optimization functions. For the remainder of the functions see Appendix C. After each iteration, the model is fitted, the most informative PC is queried, and its result is added to the dataset. It can be seen that both GP and SkewGP scale much worse on the dataset size. Comparing the running time after 200 iterations, our proposed method takes approximately 30s on both the 2D and 5D functions. GP takes approximately 1000s on Levy2D and 1700s on the 5D function. SkewGP takes around 1350s for the 2D function and almost 2900s

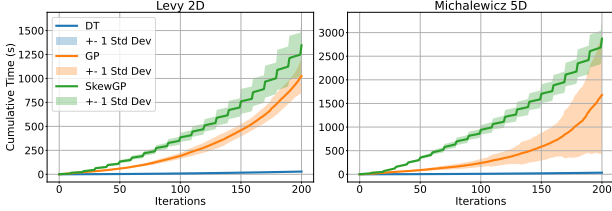


Figure 3. Running time of DT, GP, and SkewGP for the Levy2D and Michalewicz5D optimization functions.

on the 5D function. The results show that our models scales much better in dataset size and can therefore be used on much larger datasets than the GP-based alternatives.

5. Application: Sushi preference dataset

To assess the interpretability and capability of handling categorical data of our DT-based method, we apply it to the Sushi Preference dataset (Kamishima, 2003). The dataset contains item (sushi) features and user features. Users were given 10 types of sushi and were asked to rank these sushi from 1 to 10. Item features contain continuous features, such as oiliness, and categorical features, such as whether the sushi contains seafood, vegetables, meat, etc. User features contain information about the age, gender, and geographical origin of people. For a detailed overview of the features, view Appendix D. The Sushi dataset consists of two datasets: dataset A where the same 10 different sushi were tried by all users, and dataset B, which includes a subset of 10 sushi items randomly selected from 100. Originally, the dataset is a ranking, which we converted to PCs for compatibility with our model. First, as described in Section 5.1, an individual’s preferences are learned using only item features. When user features are incorporated, the model can identify a user’s preferences more efficiently by leveraging information from users with similar characteristics, as shown in Section 5.2.

5.1. Without user features

Ignoring the user features for now and resetting the decision tree for each user, the model’s goal is to find the user’s preference function in as few comparisons as possible. To measure the model’s performance, a regret function similar to the ρ -regret in Husslage et al. (2015) is taken, but instead of a top five, a top three is chosen. This regret penalizes the model when items ranked outside the top three appear within the top three. The lower the true rank of the item that enters the top three, the higher the regret. For equal estimated ranks, competition ranking (Fagin et al., 2004) is used, such that when the top three sushi fall in the same leaf, the regret is still zero; however if all sushi fall in the same leaf, the regret is high. This definition of regret is chosen due to its focus on the predictions of the top

ranked items, which, with the qEUBO acquisition function, is fairer than other ranking comparisons, such as the often chosen Kendall Tau, which focuses on the exact order of the ranking from top to bottom. Similarly, solely focusing on the single most preferred sushi says too little about the full prediction of the model. A more detailed explanation and example of the ρ -regret can be found in Appendix E. We compare the performance of our model with the qEUBO acquisition function to our model with random pairwise comparisons, and with a GP-based model with qEUBO. For the DT, comparisons that fall within the same leaf are prioritized in this application.

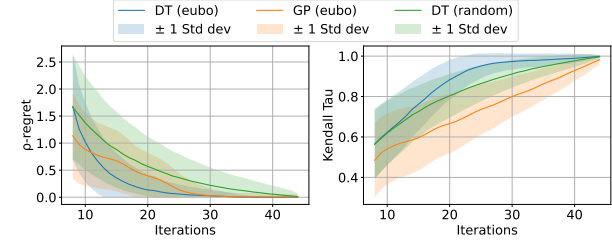


Figure 4. ρ -regret for sushi preference without user features for DT and GP. Kendall Tau is also plotted for reference.

As shown in Figure 4, DT-qEUBO obtains a slightly lower regret than GP-qEUBO. The Kendall Tau is significantly higher, even with a random acquisition function, meaning the DT is clearly better in recovering the full ranking order. However, this comparison is slightly unfair due to the prioritization of comparisons within the same leaf. The performance of the GP here is similar to the performance achieved by Nguyen et al. (2021). An example of our DT showing its interpretability is shown in Figure 5, which shows that for a user group cheaper sushi are generally less liked while akami, shrimp, or crab sushi are more liked.

5.2. With user features

Up until now, when learning the preferences of a single user the optimization process is started from blank each time. Instead, when one has access to a database of users who already completed the optimization process, one might want to use this historic data to speed up the learning process for new unseen users. Adding user features, however, presents a new problem. The consistency score is based on making splits between comparisons but comparisons are never made between users. Hence, the presented consistency score is not suitable for making splits on user features. A solution is to train a separate tree for user features, which uses a modified consistency score. Instead of leaf values, this user tree contains decision trees trained on item features from the comparisons in each leaf. While other approaches to combine user and item features exist, the mentioned approach is most interpretable, as it keeps both feature types separated

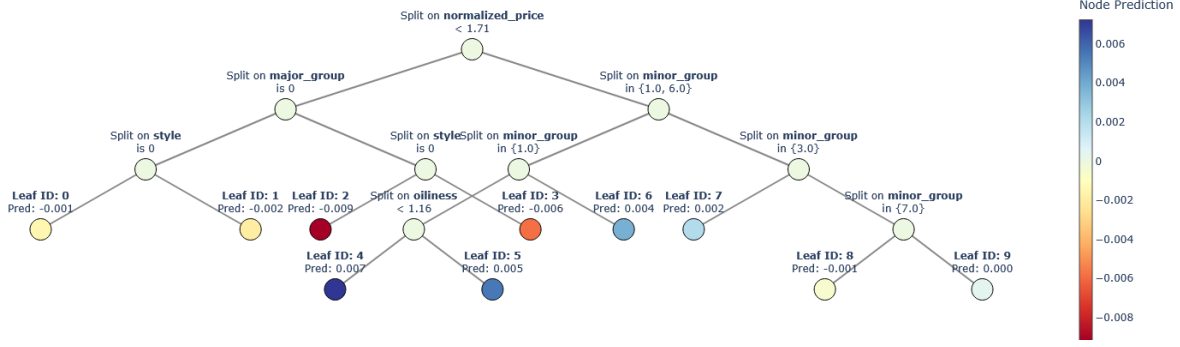


Figure 5. An example plot of an item DT for users from regions Shikoku, Tohoku or Kanto. The tree has not been post-pruned.

and reduces the dimensionality each item tree must handle, which is something our algorithm struggles with. Essentially this approach builds a user DT that partitions users in clusters of similar users based on their preferences. For each cluster of users, a regular item DT is constructed to represent their joint preferences.

The User Consistency Score defined in Equation 10 serves as the splitting criterion for the decision tree. The fundamental objective is to find splits that partition users into groups with the most internally consistent preferences. A group is considered consistent if, for any given pair of items (A, B), the users within that group strongly agree on the preference direction (i.e., most users state $A > B$ with very few stating $B > A$, or vice versa). For a given set of user comparisons D at a node, a split partitions D into two subsets, D_{left} and D_{right} . The gain G from this split is calculated as the sum of the consistency scores of the two resulting child nodes. The formula is:

$$G(k, t) = \sum_{i,j} |C(i \succ j, D_{left}) - C(j \succ i, D_{left})| + \sum_{i,j} |C(i \succ j, D_{right}) - C(j \succ i, D_{right})|. \quad (10)$$

Where $C(i \succ j)$, D_k is the count of comparisons where item i was preferred over item j within D_k . The model seeks to maximize this score, finding the split that creates child nodes with the strongest internal preference agreement.

During active learning, both the user- and the item tree are trained. The user tree determines which item tree a given user is assigned to. Then, that selected item tree is updated using the new user's data, with its prior set to the mean of the posterior obtained from the users previously assigned to that same item tree and a high uncertainty matrix to allow the tree to quickly adapt to the new user. The results for both dataset A and B are shown in Figure 6. This method of creating item trees at the leaves of user trees is not directly applicable to a GP, so the comparison with a GP is left out. For dataset A, using the posterior from previous users as the prior for item trees accelerates regret reduction, though

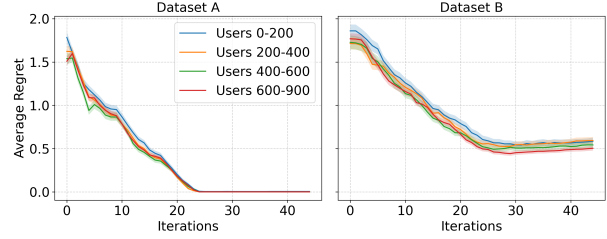


Figure 6. Average regret for 900 users as training the user tree progresses. After every 50 users, the user tree is updated. The maximum tree depth is limited to 5 for both trees. ± 1 Std. dev. is shown in the error bars for the users within these cohorts.

the time to reach zero regret remains about the same. For dataset B, the final regret decreases as the item tree grows. However, it does not reach zero because the number of leaves is limited, meaning that some of the 100 sushi items inevitably share the same leaf.

Overall, incorporating user data appears beneficial, but further refinement is needed to achieve significantly better results than the baseline without user data.

6. Conclusion

In this paper we proposed a novel tree-based surrogate model for PBO. The tree-based model, as opposed to GP-based models, is inherently interpretable, able to capture discontinuities, scalable to large datasets, and well-suited for both continuous and categorical data. Experimental results on eight increasingly spiky benchmark optimization functions show that our proposed tree-based model performs better on spiky optimization functions and only slightly worse on non-spiky functions. Additionally, by applying our model to the Sushi dataset its inherent interpretability and capability of learning an individual's preferences are highlighted. Finally, we show some initial work on using historic data to speed up the preference learning process for new unseen test-subjects. An interesting direction for future work is to allow the DM to state indifference between

a PC. Moreover, future work could look into incorporating a monotonicity constraint (e.g., lesser is always better) to the model.

Impact Statement

This paper presents work whose goal is to advance the field of Machine Learning. There are many potential societal consequences of our work, none which we feel must be specifically highlighted here.

Funding Statement

This research is funded by the Chair of Data Science, Safety & Security at Tilburg University, and NLR Royal Netherlands Aerospace Centre.

References

Astudillo, R. and Frazier, P. Multi-attribute bayesian optimization with interactive preference learning. In Chiappa, S. and Calandra, R. (eds.), *Proceedings of the Twenty Third International Conference on Artificial Intelligence and Statistics*, volume 108 of *Proceedings of Machine Learning Research*, pp. 4496–4507. PMLR, 26–28 Aug 2020. URL <https://proceedings.mlr.press/v108/astudillo20a.html>.

Astudillo, R., Lin, Z. J., Bakshy, E., and Frazier, P. queubo: A decision-theoretic acquisition function for preferential bayesian optimization. In Ruiz, F., Dy, J., and van de Meent, J.-W. (eds.), *Proceedings of The 26th International Conference on Artificial Intelligence and Statistics*, volume 206 of *Proceedings of Machine Learning Research*, pp. 1093–1114. PMLR, 25–27 Apr 2023. URL <https://proceedings.mlr.press/v206/astudillo23a.html>.

Balandat, M., Karrer, B., Jiang, D., Daulton, S., Letham, B., Wilson, A. G., and Bakshy, E. Botorch: A framework for efficient monte-carlo bayesian optimization. In Larochelle, H., Ranzato, M., Hadsell, R., Balcan, M., and Lin, H. (eds.), *Advances in Neural Information Processing Systems*, volume 33, pp. 21524–21538. Curran Associates, Inc., 2020. URL https://proceedings.neurips.cc/paper_files/paper/2020/file/f5b1b89d98b7286673128a5fb112cb9a-Paper.pdf.

Benavoli, A. and Azzimonti, D. A tutorial on learning from preferences and choices with gaussian processes. *arXiv preprint arXiv:2403.11782*, 2024.

Benavoli, A., Azzimonti, D., and Piga, D. Preferential bayesian optimisation with skew gaussian processes. In *Proceedings of the Genetic and Evolutionary Computation Conference Companion*, GECCO ’21, pp. 1842–1850, New York, NY, USA, 2021. Association for Computing Machinery. ISBN 9781450383516. doi: 10.1145/3449726.3463128. URL <https://doi-org.tilburguniversity.idm.oclc.org/10.1145/3449726.3463128>.

Brochu, E., Brochu, T., and de Freitas, N. A bayesian interactive optimization approach to procedural animation design. In *Proceedings of the 2010 ACM SIGGRAPH/Eurographics Symposium on Computer Animation*, SCA ’10, pp. 103–112, Goslar, DEU, 2010. Eurographics Association.

Cheng, W., Hühn, J., and Hüllermeier, E. Decision tree and instance-based learning for label ranking. In *Proceedings of the 26th Annual International Conference on Machine Learning*, pp. 161–168, Montreal Quebec Canada, June 2009. ACM. doi: 10.1145/1553374.1553395. URL <https://dl.acm.org/doi/10.1145/1553374.1553395>.

Chipman, H. A., George, E. I., and McCulloch, R. E. Bayesian cart model search. *Journal of the American Statistical Association*, 93(443):935–948, 1998. doi: 10.1080/01621459.1998.10473750. URL <https://doi.org/10.1080/01621459.1998.10473750>.

Chu, W. and Ghahramani, Z. Preference learning with gaussian processes. In *Proceedings of the 22nd International Conference on Machine Learning*, ICML ’05, pp. 137–144, New York, NY, USA, 2005. Association for Computing Machinery. ISBN 1595931805. doi: 10.1145/1102351.1102369. URL <https://doi-org.tilburguniversity.idm.oclc.org/10.1145/1102351.1102369>.

Eaton, M. L. *Multivariate statistics : a vector space approach*, pp. 116–117. Wiley series in probability and mathematical statistics. Wiley, New York, NY, 1983. ISBN 0471027766. doi: 10.1214/lnms/1196285102.

Fagin, R., Kumar, R., Mahdian, M., Sivakumar, D., and Vee, E. Comparing and aggregating rankings with ties. In *Proceedings of the twenty-third ACM SIGMOD-SIGACT-SIGART symposium on Principles of database systems*, pp. 47–58, Paris France, June 2004. ACM. ISBN 978-1-58113-858-0. doi: 10.1145/1055558.1055568. URL <https://dl.acm.org/doi/10.1145/1055558.1055568>.

Fauvel, T. and Chalk, M. Efficient exploration in binary and preferential bayesian optimization. *arXiv preprint arXiv:2110.09361*, 2021.

Gilboa, I., Minardi, S., and Wang, F. Consumption of values. Hec paris research paper no. eco/scd-2020-1406, HEC Paris, November 2020. URL <https://ssrn.com/abstract=3740458>.

González, J., Dai, Z., Damianou, A., and Lawrence, N. D. Preferential Bayesian optimization. In Precup, D. and Teh, Y. W. (eds.), *Proceedings of the 34th International Conference on Machine Learning*, volume 70 of *Proceedings of Machine Learning Research*, pp. 1282–1291. PMLR, 06–11 Aug 2017. URL <https://proceedings.mlr.press/v70/gonzalez17a.html>.

Greco, S., Mousseau, V., and Słowiński, R. Ordinal regression revisited: Multiple criteria ranking using a set of additive value functions. *European Journal of Operational Research*, 191(2):416–436, 2008. ISSN 0377-2217. doi: <https://doi.org/10.1016/j.ejor.2007.08.013>. URL <https://www.sciencedirect.com/science/article/pii/S0377221707008752>.

Husslage, B., Borm, P., Burg, T., Hamers, H., and Lindelauf, R. Ranking terrorists in networks: A sensitivity analysis of Al Qaeda’s 9/11 attack. *Social Networks*, 42:1–7, July 2015. ISSN 03788733. doi: 10.1016/j.socnet.2015.02.003. URL <https://linkinghub.elsevier.com/retrieve/pii/S0378873315000088>.

Kamishima, T. Nantonac collaborative filtering: recommendation based on order responses. In *Proceedings of the Ninth ACM SIGKDD International Conference on Knowledge Discovery and Data Mining*, KDD ’03, pp. 583–588, New York, NY, USA, 2003. Association for Computing Machinery. ISBN 1581137370. doi: 10.1145/956750.956823. URL <https://doi-org.tilburguniversity.idm.oclc.org/10.1145/956750.956823>.

Larichev, O. I. Cognitive validity in design of decision-aiding techniques. *Journal of Multi-Criteria Decision Analysis*, 1(3):127–138, 1992. doi: <https://doi.org/10.1002/mcda.4020010303>. URL <https://onlinelibrary.wiley.com/doi/abs/10.1002/mcda.4020010303>.

Lin, W.-A., Sung, C.-L., and Chen, R.-B. Category tree gaussian process for computer experiments with many-category qualitative factors and application to cooling system design. *Journal of Quality Technology*, 56(5):391–408, 2024. doi: 10.1080/00224065.2024.2359431. URL <https://doi.org/10.1080/00224065.2024.2359431>.

Liu, K.-H. and Shih, Y.-S. Score-scale decision tree for paired comparison data. *Statistica Sinica*, 26(1):429–444, 2016. ISSN 1017-0405. doi: 10.5705/ss.2014.164. URL <http://www3.stat.sinica.edu.tw/statistica/J26N1/J26N118/J26N118.html>.

McKay, M. D., Beckman, R. J., and Conover, W. J. A comparison of three methods for selecting values of input variables in the analysis of output from a computer code. *Technometrics*, 21(2):239–245, 1979. ISSN 00401706. URL <http://www.jstor.org/stable/1268522>.

Minka, T. P. Expectation propagation for approximate bayesian inference. In *Proceedings of the Seventeenth Conference on Uncertainty in Artificial Intelligence*, UAI’01, pp. 362–369, San Francisco, CA, USA, 2001. Morgan Kaufmann Publishers Inc. ISBN 1558608001.

Nguyen, Q. P., Tay, S., Low, B. K. H., and Jaillet, P. Top-k ranking bayesian optimization. *Proceedings of the AAAI Conference on Artificial Intelligence*, 35(10):9135–9143, May 2021. doi: 10.1609/aaai.v35i10.17103. URL <https://ojs.aaai.org/index.php/AAAI/article/view/17103>.

Nielsen, J. B. B., Nielsen, J., and Larsen, J. Perception-based personalization of hearing aids using gaussian processes and active learning. *IEEE/ACM Transactions on Audio, Speech, and Language Processing*, 23(1):162–173, 2015. doi: 10.1109/TASLP.2014.2377581.

Nuti, G., Jiménez Rugama, L. A., and Cross, A.-I. An explainable bayesian decision tree algorithm. *Frontiers in Applied Mathematics and Statistics*, 7:598833, 2021. URL <https://api.semanticscholar.org/CorpusID:232291436>.

Plate, T. A. Accuracy versus interpretability in flexible modeling: Implementing a tradeoff using gaussian process models. *Behaviormetrika*, 26(1):29–50, 1999. ISSN 1349-6964. doi: 10.2333/bhmk.26.29. URL <https://doi.org/10.2333/bhmk.26.29>.

Qomariyah, N. N., Heriyanji, E., Fajar, A. N., and Kazakov, D. Comparative Analysis of Decision Tree Algorithm for Learning Ordinal Data Expressed as Pairwise Comparisons. In *2020 8th International Conference on Information and Communication Technology (ICoICT)*, pp. 1–4, Yogyakarta, Indonesia, June 2020. IEEE. ISBN 978-1-7281-6142-6. doi: 10.1109/ICoICT49345.2020.9166341. URL <https://ieeexplore.ieee.org/document/9166341/>.

Rasmussen, C. E. and Williams, C. K. I. *Gaussian Processes for Machine Learning*. The MIT Press, 11 2005. ISBN 9780262256834. doi: 10.7551/mitpress/3206.001.0001. URL <https://doi.org/10.7551/mitpress/3206.001.0001>.

Rebelo, C. and Soares, C. Empirical Evaluation of Ranking Trees on Some Metalearning Problems. In *Proceedings 4th AAAI Multidisciplinary Workshop on Advances in Preference Handling*, 2008.

Shavarani, S. M., López-Ibáñez, M., Allmendinger, R., and Knowles, J. An interactive decision tree-based evolutionary multi-objective algorithm. In *Evolutionary Multi-Criterion Optimization: 12th International Conference, EMO 2023, Leiden, The Netherlands, March 20–24, 2023, Proceedings*, pp. 620–634, Berlin, Heidelberg, 2023. Springer-Verlag. ISBN 978-3-031-27249-3. doi: 10.1007/978-3-031-27250-9_44. URL https://doi.org.tilburguniversity.idm.oclc.org/10.1007/978-3-031-27250-9_44.

Shavarani, S. M., Golabi, M., and Idoumghar, L. Integrating active learning for improved preference modeling in tree-based interactive evolutionary multi-objective algorithms. In *2025 IEEE Congress on Evolutionary Computation (CEC)*, pp. 1–8, 2025. doi: 10.1109/CEC65147.2025.11042957.

Siivila, E., Dhaka, A. K., Andersen, M. R., González, J., Moreno, P. G., and Vehtari, A. Preferential batch bayesian optimization. In *2021 IEEE 31st International Workshop on Machine Learning for Signal Processing (MLSP)*, pp. 1–6, 2021. doi: 10.1109/MLSP52302.2021.9596494.

Surjanovic, S. and Bingham, D. Virtual library of simulation experiments: Test functions and datasets. Retrieved October 17, 2025, from <http://www.sfu.ca/~ssurjano>, 2013.

Takeno, S., Nomura, M., and Karasuyama, M. Towards practical preferential Bayesian optimization with skew Gaussian processes. In Krause, A., Brunskill, E., Cho, K., Engelhardt, B., Sabato, S., and Scarlett, J. (eds.), *Proceedings of the 40th International Conference on Machine Learning*, volume 202 of *Proceedings of Machine Learning Research*, pp. 33516–33533. PMLR, 23–29 Jul 2023. URL <https://proceedings.mlr.press/v202/takeno23b.html>.

Williams, C. and Rasmussen, C. Gaussian processes for regression. In Touretzky, D., Mozer, M., and Hasselmo, M. (eds.), *Advances in Neural Information Processing Systems*, volume 8. MIT Press, 1995. URL https://proceedings.neurips.cc/paper_files/paper/1995/file/7cce53cf90577442771720a370c3c723-Paper.pdf.

Zintgraf, L. M., Ruijters, D. M., Linders, S., Jonker, C. M., and Nowé, A. Ordered preference elicitation strategies for supporting multi-objective decision making. In *Proceedings of the 17th International Conference on Autonomous Agents and MultiAgent Systems*, AAMAS '18, pp. 1477–1485, Richland, SC, 2018. International Foundation for Autonomous Agents and Multiagent Systems.

A. Removing Translational Degeneracy

The pairwise likelihood defined in Equation 2 is *translationally invariant* with respect to \mathbf{f} . That is, adding a constant shift c to all components of \mathbf{f} does not influence the pairwise differences and thus leaves the likelihood unchanged. Intuitively, this invariance is expected: because the latent function f is never observed directly, its absolute scale is unidentifiable. However, this invariance has a direct consequence for the Hessian of $L(\mathbf{f})$ and therefore for the posterior covariance defined in Equation 8. In particular, the likelihood Hessian term Λ_{MAP} is *degenerate* in the constant shift direction: $\Lambda_{\text{MAP}}\mathbf{1} = \mathbf{0}$, where $\mathbf{1}$ is the m -dimensional all-ones vector and $\mathbf{0}$ the m -dimensional all-zeroes vector.

As a result, the curvature of the negative log-posterior in the all-ones direction, $\mathbf{1}^\top H(L(\mathbf{f}))\mathbf{1}$, is governed entirely by the prior:

$$\mathbf{1}^\top H(L(\mathbf{f}))\mathbf{1} = \mathbf{1}^\top \left(\frac{1}{\sigma_{\text{prior}}^2} I + \Lambda_{\text{MAP}} \right) \mathbf{1} = \frac{m}{\sigma_{\text{prior}}^2}.$$

Consequently, the posterior covariance in this direction is:

$$\mathbf{1}^\top \Sigma_{\text{post}} \mathbf{1} = \mathbf{1}^\top H(L(\mathbf{f}))^{-1} \mathbf{1} = m\sigma_{\text{prior}}^2.$$

which follows from solving the linear system $H(L(\mathbf{f}))\mathbf{v} = \mathbf{1}$, which implies $\mathbf{v} = H(L(\mathbf{f}))^{-1}\mathbf{1}$. Since $H(L(\mathbf{f}))\mathbf{1} = \frac{1}{\sigma_{\text{prior}}^2}\mathbf{1}$, it follows that $\mathbf{v} = \sigma_{\text{prior}}^2 \mathbf{1}$.

This invariance causes two problems. First, it introduces a large irreducible variance term $m\sigma_{\text{prior}}^2$, especially when σ_{prior} is large. Second, it can cause a singular or ill-conditioned Hessian. For a weak prior (large σ_{prior}^2), the curvature in the all-ones direction becomes nearly flat making the Hessian singular. Besides that, increasing the number of data points n can also cause severe ill-conditioning. The curvature of the likelihood typically grows with n , since more data provide more information. However, the all-ones direction remains unaffected by the data due to translational invariance. As a result, the eigenvalues of the Hessian become increasingly disparate as n grows: the largest eigenvalues scale with n , while the smallest remains at $\frac{m}{\sigma_{\text{prior}}^2}$. Thus making the Hessian ill-conditioned for large n and/or large σ_{prior}^2 . In practice, this causes numerical instability even when the Hessian is formally invertible. Note that both of these problems also exist for GP priors, severely hindering the numerical stability of the Hessian inversions.

To remove the irreducible variance and prevent numerical issues with the Hessian, the model is made identifiable by adding a sum-to-zero constraint: $\sum_{i=1}^m f_i = \mathbf{1}\mathbf{f} = 0$. Essentially, this fixes the scale of the model, preventing a shift in the all-ones-direction, and thereby removing any variance coming from this direction. This constraint is incorporated by conditioning the posterior on $\mathbf{1}\mathbf{f} = 0$. The posterior then follows a conditional distribution $p(\mathbf{f}|\mathbf{1}\mathbf{f} = 0, \mathcal{D})$. Note that since $p(\mathbf{f}|\mathcal{D})$ follows a normal distribution after Laplace approximation, $p(\mathbf{f}|\mathcal{D})$ also follows a normal distribution (as a sum of normal distributions), and thus by using Eaton's (Eaton, 1983) normal conditional distribution result $p(\mathbf{f}|\mathbf{1}\mathbf{f} = 0, \mathcal{D})$ follows a conditional normal distribution (for the full derivation see below).

Derivation of the Conditional Distribution We start from Eaton's general result (Eaton, 1983, pp. 116–117) for the conditional distribution of a joint normal vector

$$\begin{pmatrix} X \\ S \end{pmatrix} \sim \mathcal{N}\left(\begin{pmatrix} \boldsymbol{\mu} \\ \boldsymbol{\mu}_S \end{pmatrix}, \begin{pmatrix} \Sigma_{11} & \Sigma_{12} \\ \Sigma_{21} & \Sigma_{22} \end{pmatrix}\right),$$

where $X \in \mathbb{R}^n$, $S \in \mathbb{R}$,

then $X \mid (S = s)$ follows a multivariate normal

$$X \mid (S = s) \sim \mathcal{N}\left(\boldsymbol{\mu} + \Sigma_{12} \Sigma_{22}^{-1} (s - \boldsymbol{\mu}_S), \Sigma_{11} - \Sigma_{12} \Sigma_{22}^{-1} \Sigma_{21}\right).$$

Specializing to the Sum Constraint

Let

$$T = (1, 1, \dots, 1)^\top = \mathbf{1} \in \mathbb{R}^n, \quad S = T^\top X = \sum_{i=1}^n X_i, \quad \mu_S = T^\top \mu = \sum_{i=1}^n \mu_i, \quad s = 0$$

Note that S is normally distributed as it is the sum of normally distributed random variables. Also note that (X_1, \dots, X_N, S) is jointly normal as an affine transform of a jointly normal distribution. Therefore, we can use Eaton's result with the following covariance blocks:

(i) Σ_{12} .

$$\Sigma_{12} = \text{Cov}(X, T^\top X) = \text{Cov}\left(X, \sum_{i=1}^n T_i X_i\right) \stackrel{\text{bilinearity}}{=} \sum_{i=1}^n T_i \text{Cov}(X, X_i) = \sum_{i=1}^n T_i \Sigma_{:,i} = \Sigma T.$$

(ii) Σ_{21} .

$$\Sigma_{21} = \text{Cov}(T^\top X, X) = T^\top \text{Cov}(X, X) = T^\top \Sigma = (\Sigma T)^\top$$

(iii) Σ_{22} .

$$\Sigma_{22} = \text{Var}(T^\top X) = T^\top \Sigma T,$$

which is a scalar. Its inverse is thus simply $\Sigma_{22}^- = \frac{1}{T^\top \Sigma T}$.

Plugging into the Block-Formula

Using these identifications in the conditional-normal formula, gives

$$X \mid \sum_{i=1}^n X_i = 0 \sim \mathcal{N}\left(\mu - \frac{T^\top \mu}{T^\top \Sigma T} \Sigma T, \Sigma - \frac{1}{T^\top \Sigma T} (\Sigma T)(\Sigma T)^\top\right).$$

B. Surface Plots of optimization functions

In Figure 7, surface plots of eight benchmark optimization functions used in the experiments in Section 4 are shown. For Rosenbrock, Michalewicz, and Schwefel, 2D variants of the functions have been plotted. For Hartmann, an arbitrarily chosen 2D slice ($z = 0.7$) of the 3D variant has been shown. The surface plots show that the eight optimization functions are increasingly spiky from left to right, top to bottom. In particular, both the amount of spikes and the individual strength of spikes increase. Further details about the optimization functions can be found in [Surjanovic & Bingham \(2013\)](#). Note that the original functions are all minimization functions, however, since our model tries to find the maximum, the functions are all transformed by multiplying them with -1 .

C. Time plots

Looking at Figure 8, both GP and SkewGP scale much worse with dataset size than DT. Note that the standard deviation of the running time of GP is quite high for Branin and De Jong. In both these cases, the GP struggled with numerically unstable matrix inversions which increased the running time. For all functions the running time of DT is approximately 30s, whereas the GP and SkewGP methods take much longer.

D. Sushi dataset details

The sushi dataset consists of both item features and user features. The item features can be found in Table 1, and the user features can be found in Table 2.

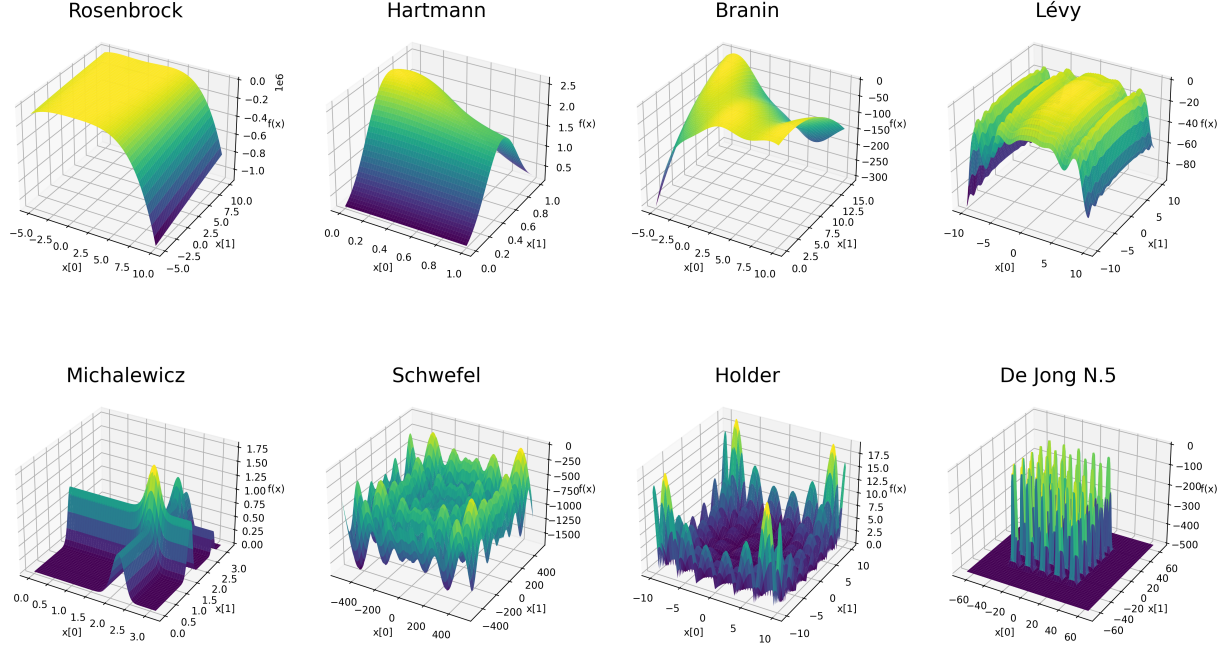


Figure 7. Surface plots of each optimization function. The functions are ordered from left to right, top to bottom in increasing order of "spikiness". "Spikiness" refers to both the frequency and the strength of sudden changes (i.e. spikes) in the function values.

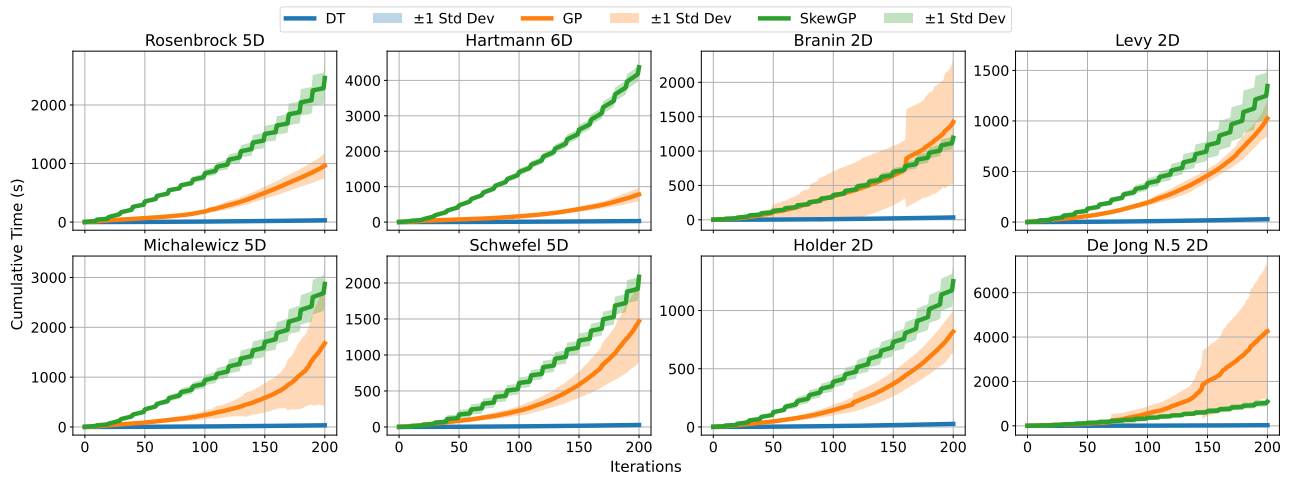


Figure 8. Running time for each benchmark optimization function for DT, GP and SkewGP.

Table 1. Item features of the sushi dataset.

Name	Type	Range
Style	binary	{0, 1}
Major group	binary	{0, 1}
Minor group	categorical	{0, ..., 11}
Oiliness	continuous	[0, 4]
Frequently eat	continuous	[0, 3]
Normalized price	continuous	[0, 1]

Table 2. User features of the sushi dataset.

Name	Type	Range
Gender	binary	{0, 1}
Age	categorical	{0, 5}
Time	continuous	[0, 1500]
Prefecture (< 15)	categorical	{0, ..., 47}
Region (< 15)	categorical	{0, ..., 11}
E/W (< 15)	binary	{0, 1}
Prefecture (curr)	categorical	{0, ..., 47}
Region (curr)	categorical	{0, ..., 11}
E/W (curr)	binary	{0, 1}
Prefecture chg	binary	{0, 1}

E. Rho-regret calculation

The ρ -regret is defined as the difference between ranking R_{pred} and R_{true} represented by $\rho(R_{true}, R_{pred}) \geq 0$. Each item is assigned a value based on its position in the ranking, which values are shown in Table 3. The regret is then defined as the sum of the values of all items that leave the top-3 from R_{true} and enter the top in R_{pred} . When highly ranked values leave the top-3 or when lowly ranked values enter the top-3, this will result in a high regret. The maximum value the regret can take would be: $\rho_{regret_{max}} = (1 + 2/3 + 1/3) + (5/7 + 6/7 + 1) = 6/3 + 18/7 \approx 4.57$.

Table 3. Values assigned to each ranking which is used to calculate the regret.

Position	1	2	3	4	5	6	7	8	9	10
Value	1	2/3	1/3	1/7	2/7	3/7	4/7	5/7	6/7	1